



耶鲁大学-南京信息工程大学大气环境中心

Yale-NUIST Center on Atmospheric Environment

# Study on the characteristic of water-soluble ion in PM<sub>2.5</sub> of Nanjing based on on-line monitoring

Zhang Yuanyuan

2016.7.15

# Outline

- Introduction
- Experimental
- Results and discussion
- Conclusions

# Introduction

- Haze pollution caused by particulate matter suspended in the air remains a major environmental issue because of its substantial impacts on climate, air quality, and human health.
- Water soluble inorganic ions (WSII) were found to be the major components of  $PM_{2.5}$ , especially secondary inorganic ions (sulfate, nitrate and ammonium) , which accounted for one third or more of  $PM_{2.5}$  (Cao et al.,2012; Kong et al., 2014).
- The most commonly used procedures for collecting aerosols are filter-based methods, but because of their low accuracy it is not simple to quantify ambient aerosols.
- Online analyzer with highly temporal resolution for monitoring aerosols and gases (MARGA) have been developed to solve the problems related to filter-base methods (Acker et al., 2005) . The characteristics of water soluble ions in Nanjing based on the results of MARGA were analyzed in this study.

# Experimental

- Site : Meteorological observation field, NUIST
- Samples: PM<sub>2.5</sub>

Table 1 Summary of data and corresponding instruments

Parameter	Duration	Instruments
1. Gases(NH <sub>3</sub> , HNO <sub>2</sub> , HNO <sub>3</sub> , HCl, SO <sub>2</sub> ) 2. Aerosols ions(NH <sub>4</sub> <sup>+</sup> , Na <sup>+</sup> , K <sup>+</sup> , Ca <sup>2+</sup> , Mg <sup>2+</sup> , Cl <sup>-</sup> , NO <sub>3</sub> <sup>-</sup> , SO <sub>4</sub> <sup>2-</sup> )	Spring:2016.3.3-2016.5.16 Summer:2016.7.11-2016.9.14 Winter:2017.1.15-2017.2.28	MARGA(ADI 2080, Applikon Analytical B. B. Corp., The Netherlands )
Mass concentration of PM <sub>2.5</sub>	2016.3.1-2017.2	THERMO (TEOM1405-DF, Thermo Scientific, USA)
Meteorological parameters (T, RH, WD,WS, P, visibility)	2016.3.1-2017.2	Vaisala (Meteorological observation field, NUIST)

# Results and discussion

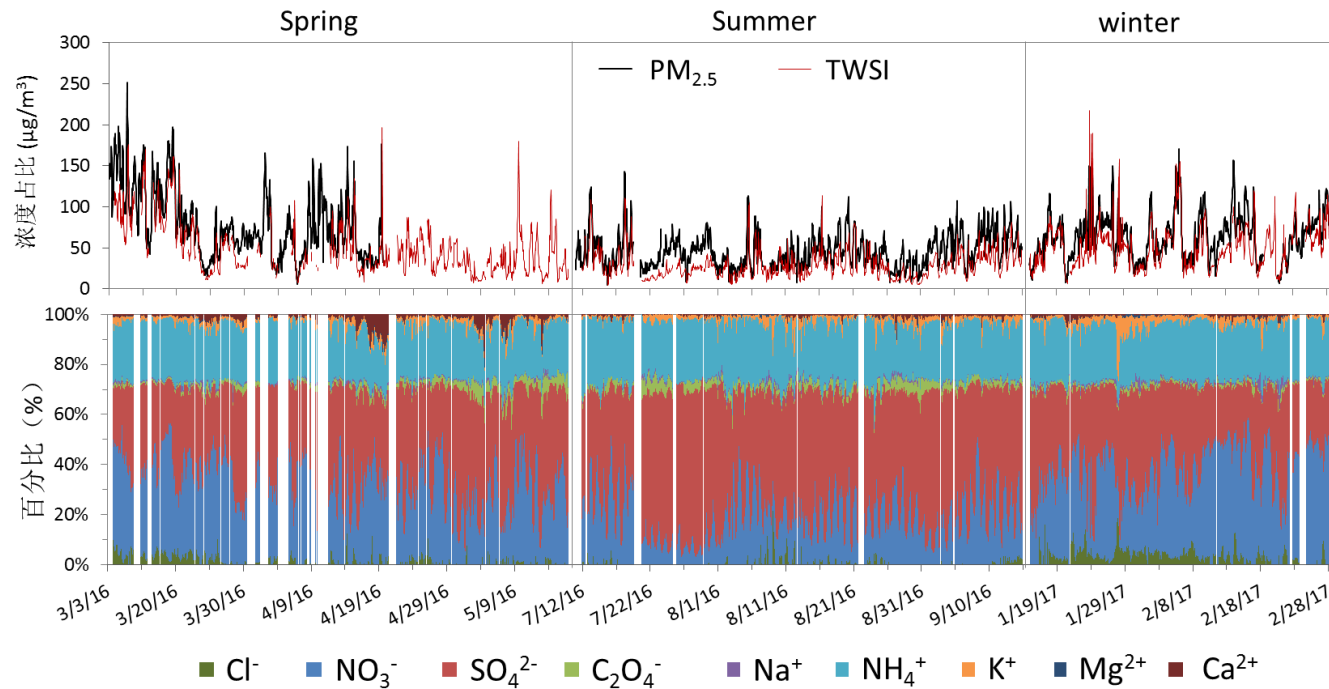


Fig 1. Time series of mass concentration ( $\mu\text{g}/\text{m}^3$ ) of PM<sub>2.5</sub>, total water-soluble ions(TWSI) and the proportion of water-soluble ions

# Results and discussion

- Seasonal variation

Table 2. Statistics of ions in different seasons

参数	春季 (2016)		夏季 (2016)		冬季 (2017)	
	浓度 (μg/m <sup>3</sup> )	占比	浓度 (μg/m <sup>3</sup> )	占比	浓度 (μg/m <sup>3</sup> )	占比
Cl <sup>-</sup>	1.70	3.54%	0.42	1.47%	2.01	3.87%
NO <sub>3</sub> <sup>-</sup>	16.89	35.21%	6.83	23.63%	19.80	38.23%
SO <sub>4</sub> <sup>2-</sup>	15.87	33.09%	13.10	45.31%	15.52	29.97%
Oxalate	0.78	1.62%	0.65	2.26%	0.51	0.99%
Na <sup>+</sup>	0.28	0.59%	0.14	0.48%	0.38	0.73%
NH <sub>4</sub> <sup>+</sup>	11.01	22.95%	7.08	24.48%	11.97	23.11%
K <sup>+</sup>	0.88	1.84%	0.53	1.83%	1.22	2.35%
Mg <sup>2+</sup>	0.07	0.15%	0.02	0.09%	0.08	0.16%
Ca <sup>2+</sup>	0.58	1.20%	0.13	0.46%	0.24	0.47%
TWSI	47.96		28.91		51.79	
TWSI/PM <sub>2.5</sub> (%)	74.16		64.12		81.96	
HCl	0.01		0.20		0.00	
HNO <sub>2</sub>	2.33		2.98		2.90	
HNO <sub>3</sub>	0.85		1.04		0.92	
SO <sub>2</sub>	17.50		16.23		12.49	
NH <sub>3</sub>	13.95		18.08		9.91	
T (°C)	16.8		29.1		5.6	
RH (%)	64		68		62	

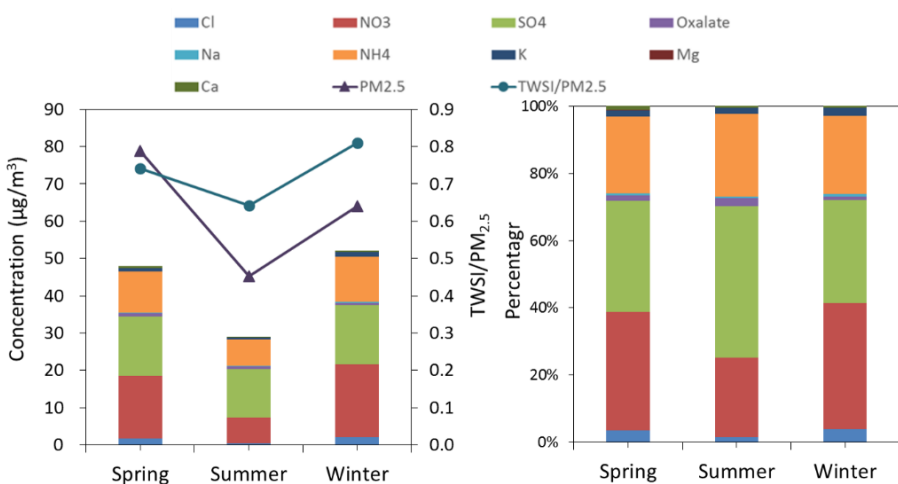


Fig 2. water-soluble ions in PM<sub>2.5</sub> in different seasons

# Introduction

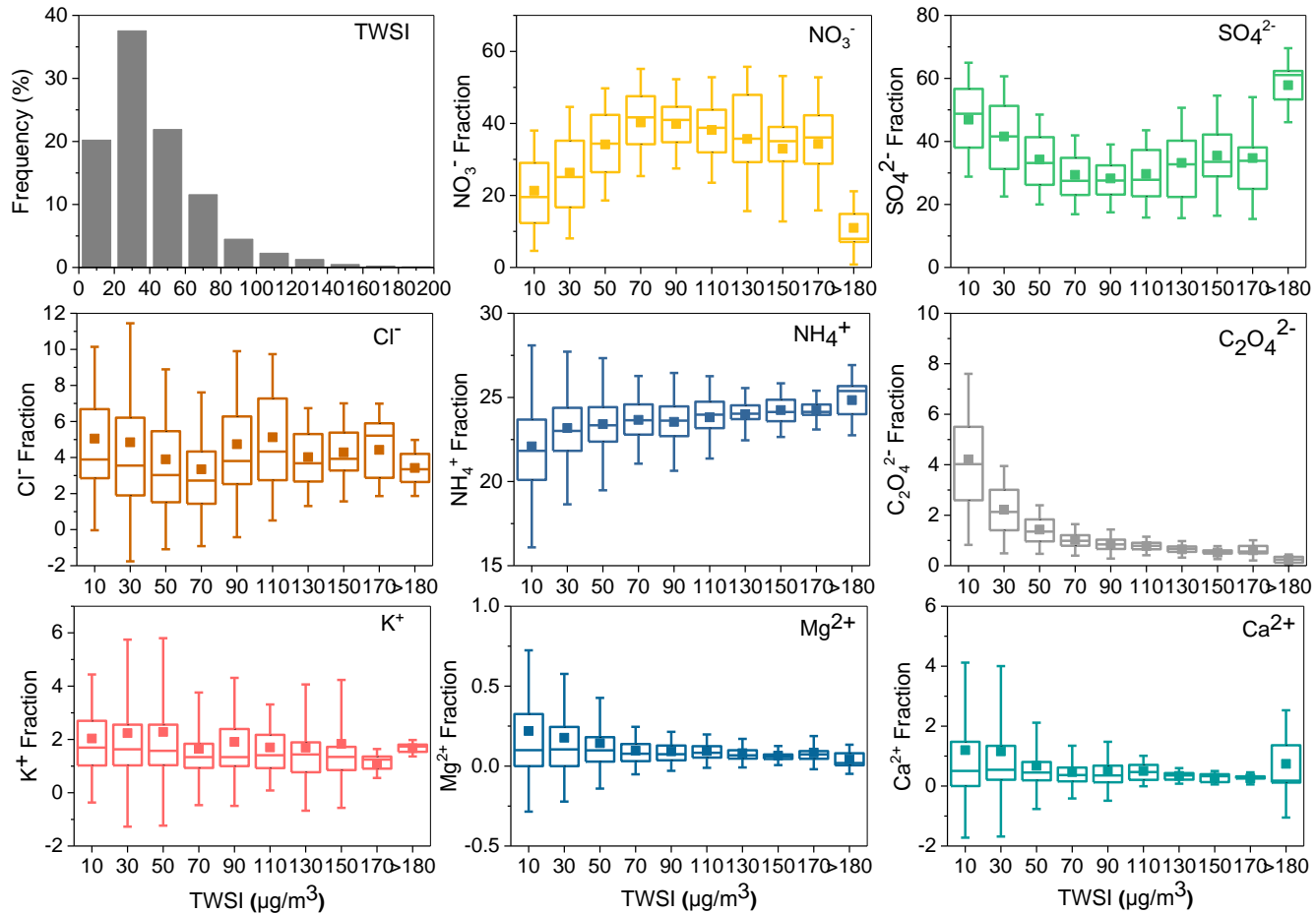


Fig.3 The variability of water-soluble ion fraction (%) and probability of total mass concentration (%)

# Results and discussion

- Diurnal variations

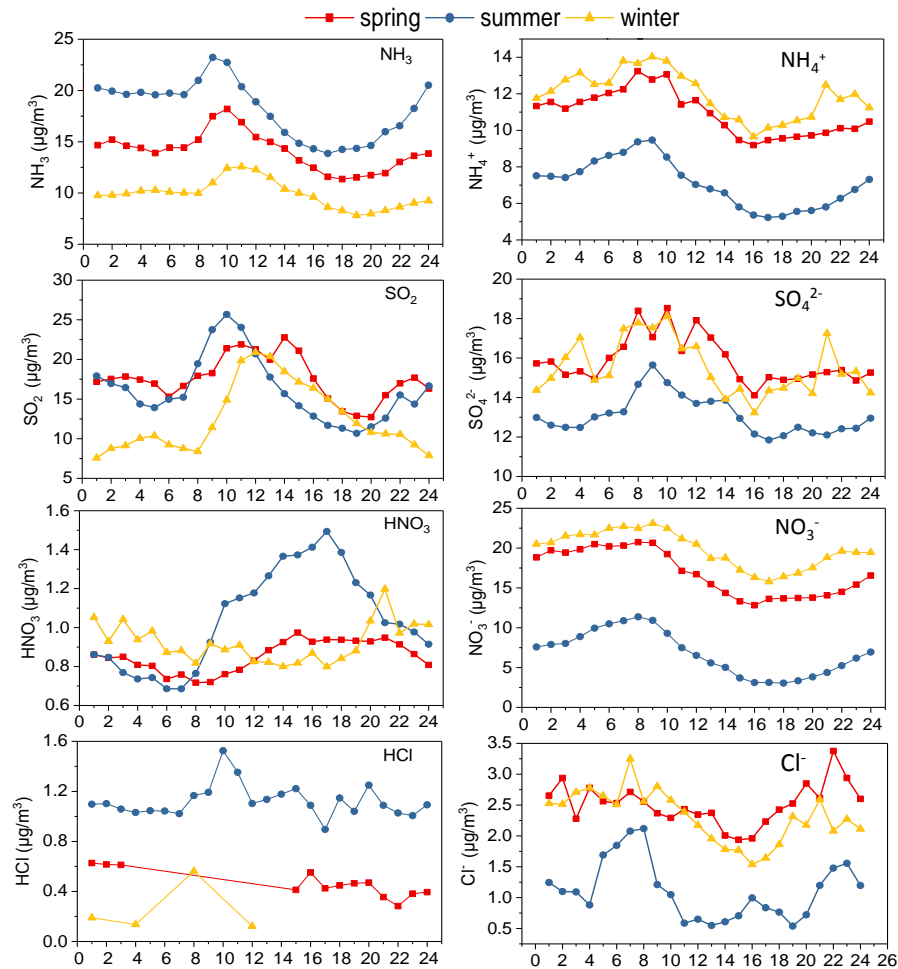


Fig 4. Diurnal variations of NH<sub>3</sub>, SO<sub>2</sub>, HNO<sub>3</sub>, and HCl and major ionic constituents in PM<sub>2.5</sub>

# Results and discussion

- Diurnal variations

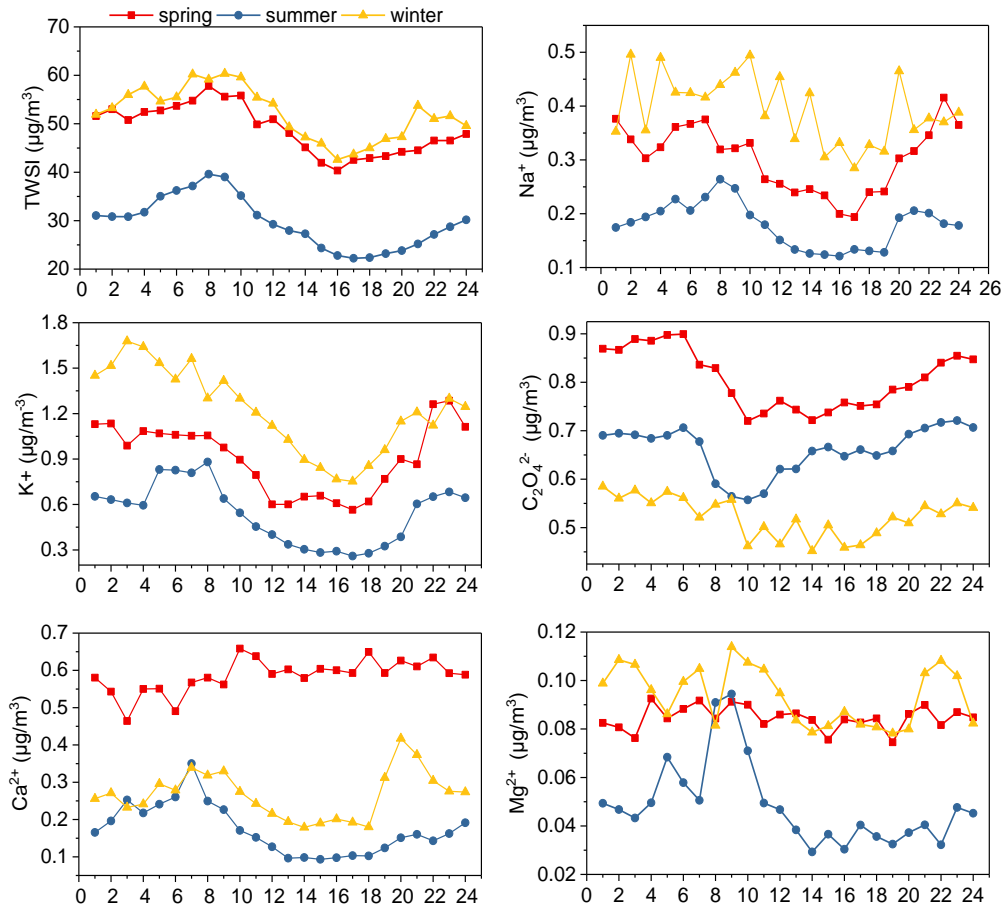


Fig 5. Diurnal variations of TWSI, and other ionic constituents in PM<sub>2.5</sub>

# Results and discussion

- Backward trajectory Cluster analysis

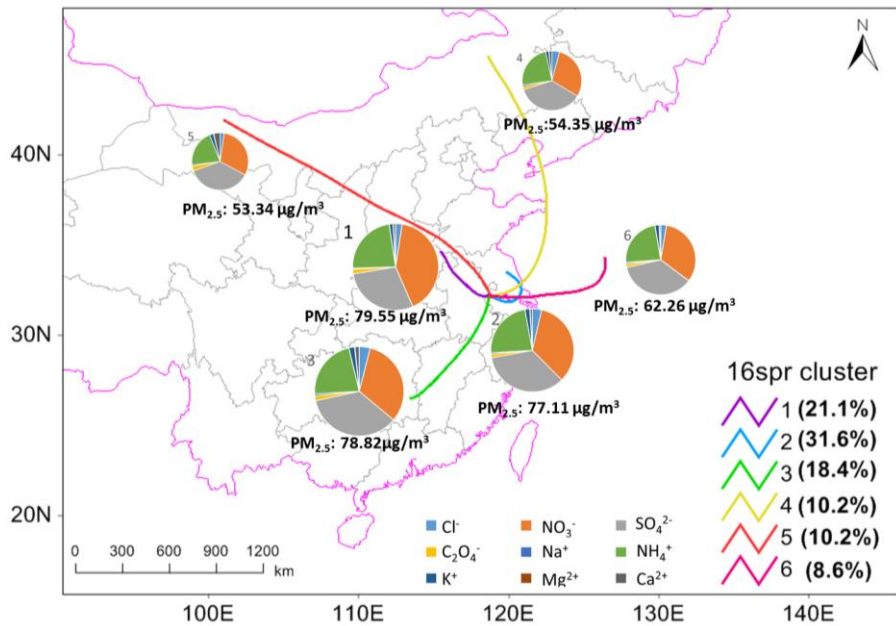


Table 3. Characteristics of source air mass in Spring

	Cluster1	Cluster2	Cluster3	Cluster4	Cluster5	Cluster6
Ratio	21.10%	31.60%	18.40%	10.20%	10.20%	8.60%
Cl <sup>-</sup>	1.21±1.92	1.86±2.75	1.81±2.36	1.52±1.82	0.73±1.22	1.04±0.95
NO <sub>3</sub> <sup>-</sup>	19.94±16.1 9	17.56±11.7 5	14.62±10.7 7	10.89±11.3 5	9.68±7.50	12.79±6.85
SO <sub>4</sub> <sup>2-</sup>	14.14±6.03	17.89±13.3 1	16.22±10.5 8	13.45±10.1 1	11.76±7.09	14.25±4.94
C <sub>2</sub> O <sub>4</sub> <sup>-</sup>	0.83±0.35	0.70±0.38	0.77±0.26	0.65±0.30	0.87±0.25	0.60±0.30
Na <sup>+</sup>	0.17±0.15	0.30±0.28	0.33±0.20	0.34±0.50	0.22±0.23	0.30±0.35
NH <sub>4</sub> <sup>+</sup>	11.26±7.46	11.89±8.18	10.11±7.23	8.81±7.20	6.63±4.22	9.23±2.73
K <sup>+</sup>	0.69±0.59	0.96±1.09	0.94±0.72	0.61±0.50	0.70±0.63	0.76±0.79
Mg <sup>2+</sup>	0.05±0.04	0.07±0.07	0.06±0.05	0.09±0.06	0.09±0.08	0.03±0.03
Ca <sup>2+</sup>	0.42±0.35	0.46±0.55	0.70±0.92	0.56±0.48	1.14±1.33	0.26±0.29
PM <sub>2.5</sub>	79.55±39.8 9	77.11±37.9 1	78.82±35.4 9	54.35±35.3 5	53.34±19.3 7	62.26±23.0 2

Fig 6. Backward trajectory Cluster analysis in Spring

# Results and discussion

- Backward trajectory Cluster analysis

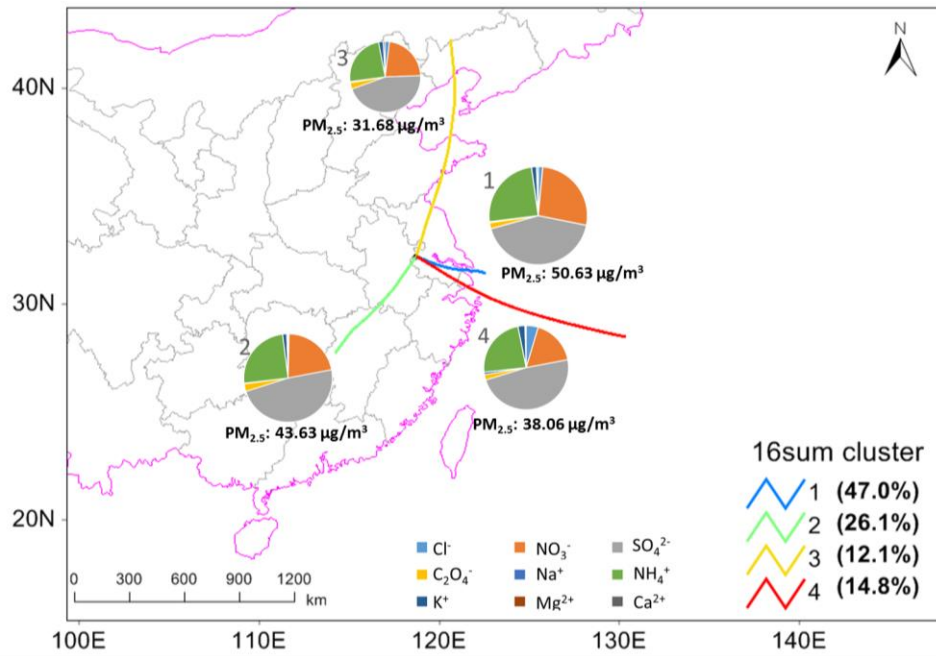


Table 4. Characteristics of source air mass in Summer

	Cluster1	Cluster2	Cluster3	Cluster4
Ratio	47.00%	26.10%	12.10%	14.80%
Cl <sup>-</sup>	0.52±1.18	0.10±0.29	0.40±0.81	1.18±2.12
NO <sub>3</sub> <sup>-</sup>	9.30±7.94	5.52±7.56	4.62±3.28	4.45±3.83
SO <sub>4</sub> <sup>2-</sup>	14.84±6.15	12.30±5.21	9.26±5.99	12.36±6.12
C <sub>2</sub> O <sub>4</sub> <sup>2-</sup>	0.69±0.23	0.71±0.33	0.60±0.15	0.53±0.18
Na <sup>+</sup>	0.12±0.12	0.07±0.07	0.11±0.10	0.25±0.18
NH <sub>4</sub> <sup>+</sup>	8.64±4.49	3.36±4.30	4.95±3.66	6.04±3.60
K <sup>+</sup>	0.58±0.52	0.39±0.27	0.43±0.61	0.68±1.15
Mg <sup>2+</sup>	0.02±0.04	0.01±0.03	0.03±0.03	0.04±0.07
Ca <sup>2+</sup>	0.17±0.23	0.11±0.21	0.16±0.35	0.08±0.11
PM <sub>2.5</sub>	50.63±22.31	43.63±17.83	31.68±14.15	38.06±13.42

Fig 7. Backward trajectory Cluster analysis in Summer

# Results and discussion

- Backward trajectory Cluster analysis

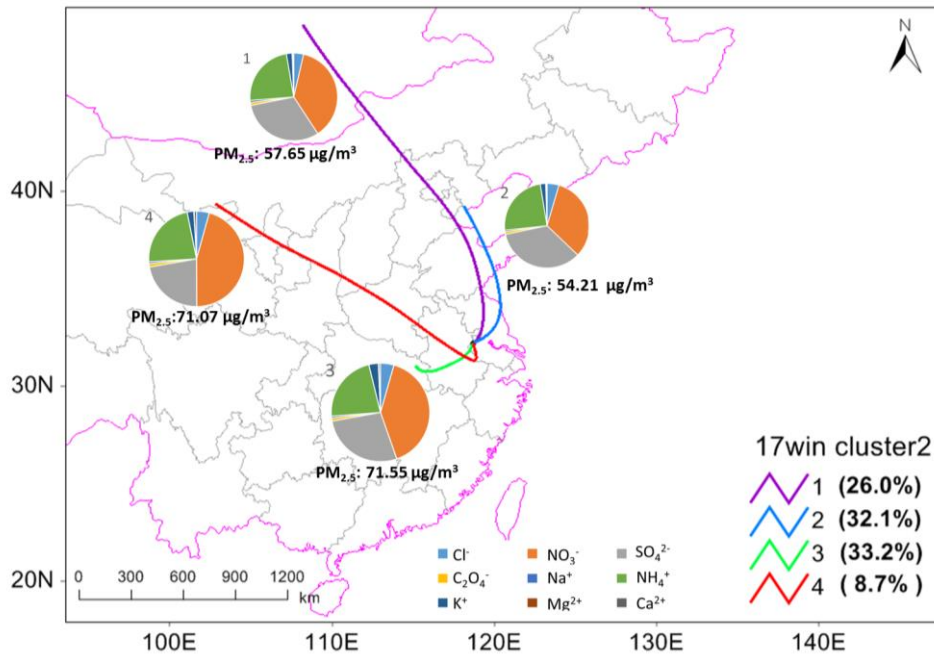


Table 5. Characteristics of source air mass in Winter

	Cluster1	Cluster2	Cluster3	Cluster4
Ratio	21.10%	31.60%	18.40%	10.20%
Cl-	1.75±1.51	2.13±1.56	2.51±3.09	2.32±1.82
NO3-	17.97±14.51	15.35±9.40	22.98±10.82	24.49±11.35
SO42-	15.07±11.91	16.23±10.54	15.74±12.47	11.98±10.11
C2O4-	0.50±0.32	0.46±0.26	0.55±0.27	0.59±0.30
Na+	0.38±0.24	0.29±0.20	0.36±0.23	0.35±0.50
NH4+	11.41±8.7	11.36±6.14	12.79±5.34	12.26±7.20
K+	1.02±0.76	0.96±0.73	1.77±2.08	1.20±0.50
Mg2+	0.09±0.08	0.07±0.07	0.09±0.1	0.08±0.06
Ca2+	0.02±0.19	0.17±0.16	0.32±0.36	0.41±0.48
PM2.5	57.65±35.84	54.21±21.80	71.55±23.88	71.07±35.35

Fig 8. Backward trajectory Cluster analysis in Winter

# Results and discussion

- Acidity of particles

$$CE = \frac{Na^+}{23} + \frac{NH_4^+}{18} + \frac{K^+}{39.1} + \frac{2 \cdot Mg^{2+}}{243} + \frac{2 \cdot Ca^{2+}}{40}$$
$$AE = \frac{Cl^-}{35.45} + \frac{2 \cdot SO_4^{2-}}{96} + \frac{NO_3^-}{62} + \frac{2 \cdot C_2O_4^{2-}}{88}$$

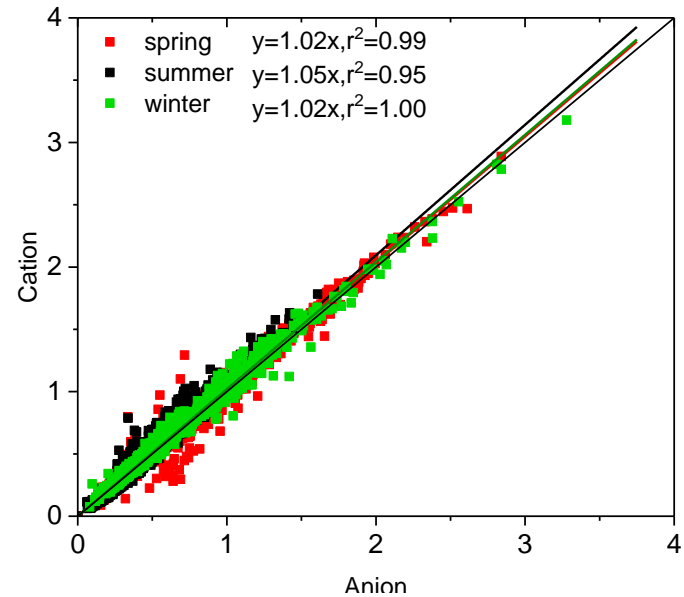


Fig 9. Backward trajectory Cluster analysis in Winter

# Results and discussion

- Backward trajectory Cluster analysis

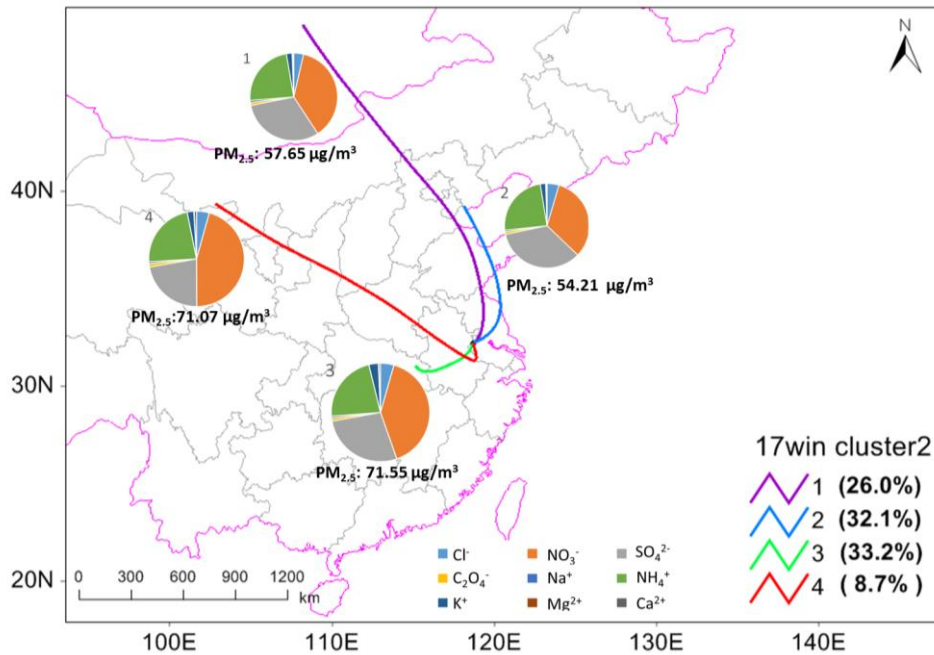


Fig 10. Backward trajectory Cluster analysis in Winter

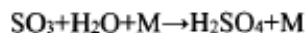
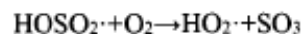
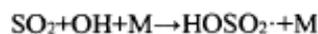
Table 5. Characteristics of source air mass in Winter

	Cluster1	Cluster2	Cluster3	Cluster4
Ratio	21.10%	31.60%	18.40%	10.20%
Cl-	1.75±1.51	2.13±1.56	2.51±3.09	2.32±1.82
NO3-	17.97±14.51	15.35±9.40	22.98±10.82	24.49±11.35
SO42-	15.07±11.91	16.23±10.54	15.74±12.47	11.98±10.11
C2O4-	0.50±0.32	0.46±0.26	0.55±0.27	0.59±0.30
Na+	0.38±0.24	0.29±0.20	0.36±0.23	0.35±0.50
NH4+	11.41±8.7	11.36±6.14	12.79±5.34	12.26±7.20
K+	1.02±0.76	0.96±0.73	1.77±2.08	1.20±0.50
Mg2+	0.09±0.08	0.07±0.07	0.09±0.1	0.08±0.06
Ca2+	0.02±0.19	0.17±0.16	0.32±0.36	0.41±0.48
PM2.5	57.65±35.84	54.21±21.80	71.55±23.88	71.07±35.35

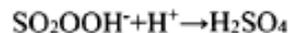
# Results and discussion

- Generation and Evolution of  $\text{SO}_4^{2-}$

(1) Gas-phase oxidation reaction



(2) Liquid chemical reaction



(3) The sulfur oxidation ratio (SOR): are available indicators used to quantitatively characterize the secondary transformation reactions of  $\text{SO}_2$ . (Yang Shi, 2012)

$$\text{SOR} = n - [\text{SO}_4^{2-}] / n - [\text{SO}_4^{2-} + \text{SO}_2]$$

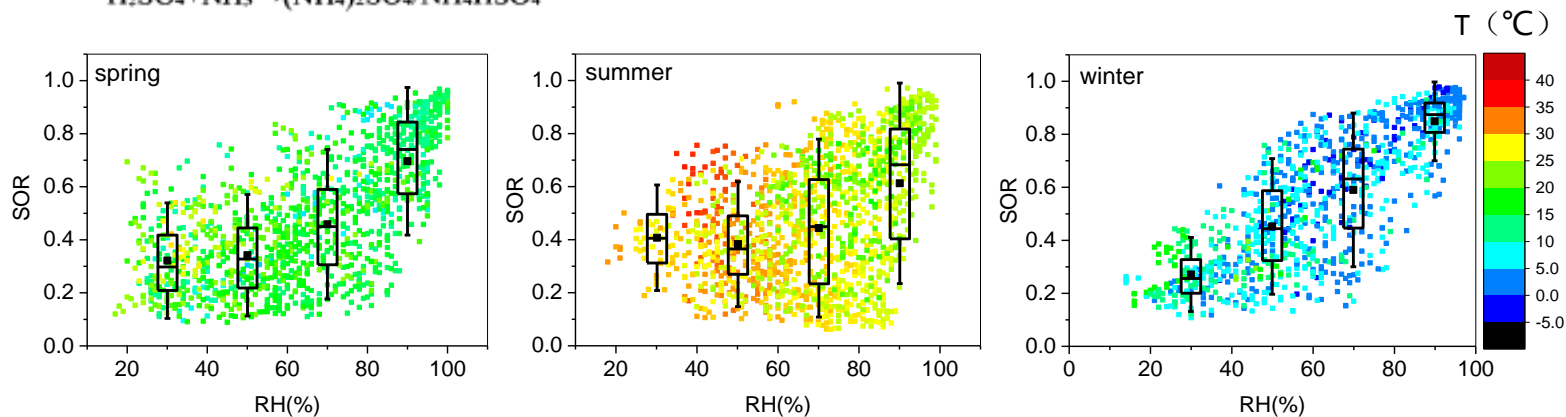


Fig 11. The relationship between SOR and RH/ T in each season

# Results and discussion

- Generation and Evolution of  $\text{SO}_4^{2-}$

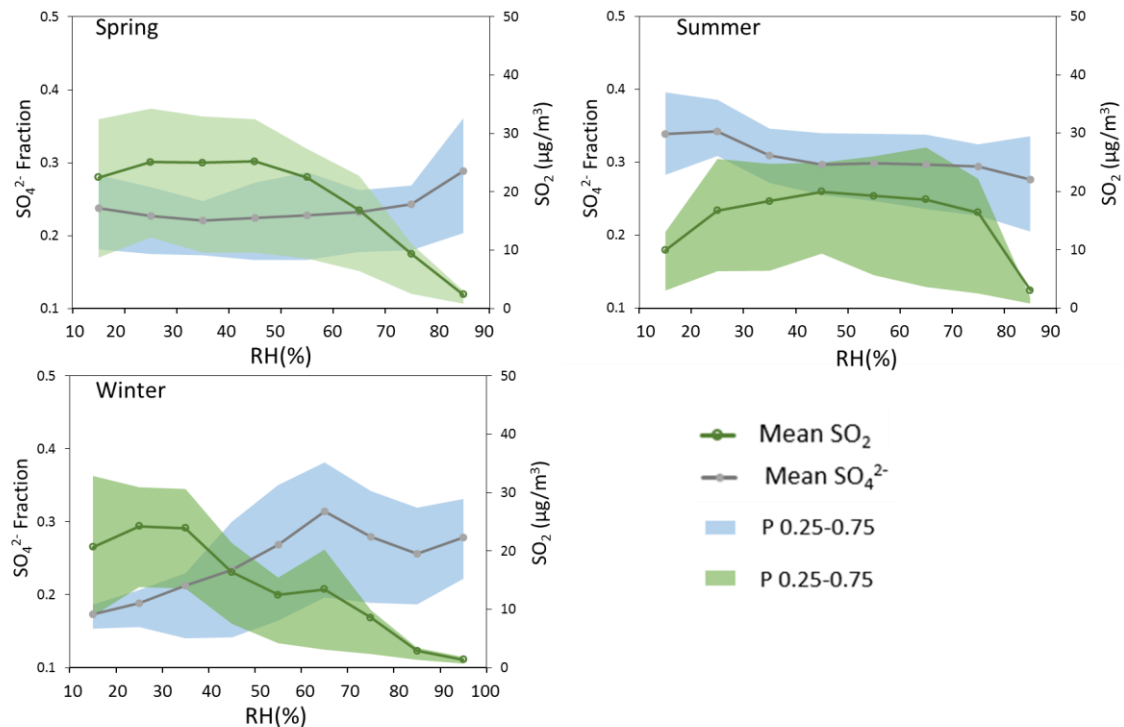


Fig 12. The relationship between fraction of  $\text{SO}_4^{2-}$  in  $\text{PM}_{2.5}$ , the concentration of  $\text{SO}_2$  and RH

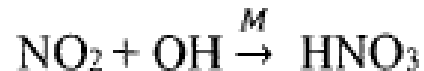
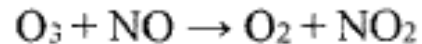
# Results and discussion

- Effect of  $T$  and RH on  $\text{NH}_4\text{NO}_3$  Gas-Particle Distribution

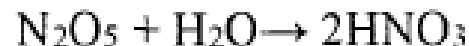
(1) Gas-phase oxidation reaction



Daytime:



Nighttime:



(2) Heterogeneous reaction: Mainly occurs at the sea salt surface



# Results and discussion

- $[\text{NO}_3^-]/[\text{SO}_4^{2-}] / [\text{NH}_4^+]/[\text{SO}_4^{2-}]$

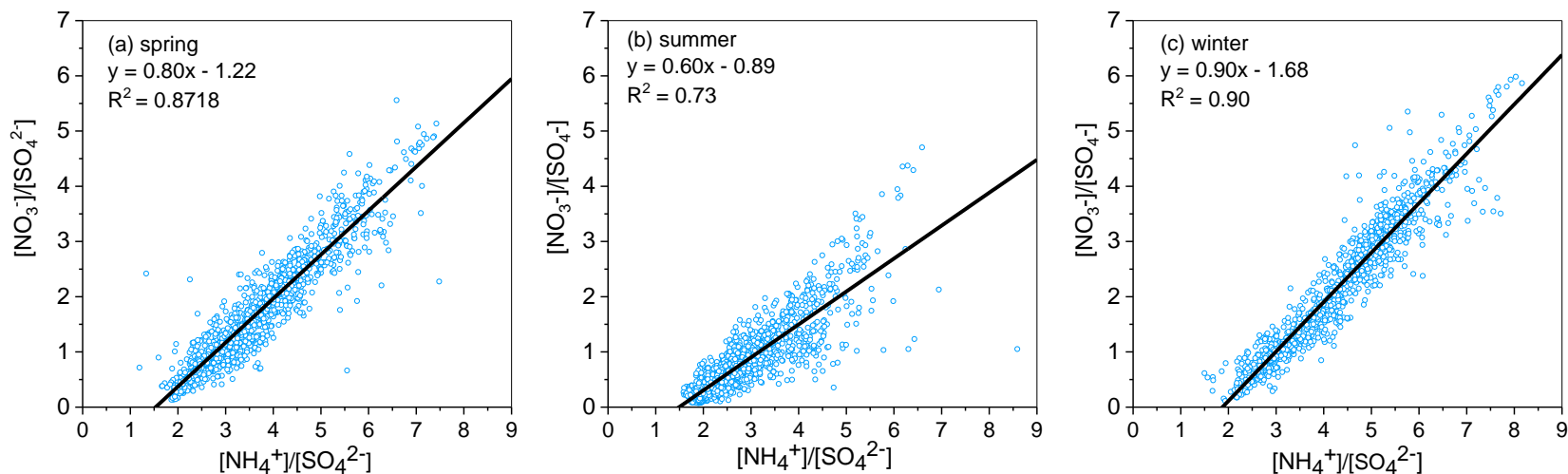


Fig 13. Relationship between  $[\text{NO}_3^-]/[\text{SO}_4^{2-}]$  and  $[\text{NH}_4^+]/[\text{SO}_4^{2-}]$

Total fitting result :  $Y=0.81x-1.37$ ,  $R^2=0.88$

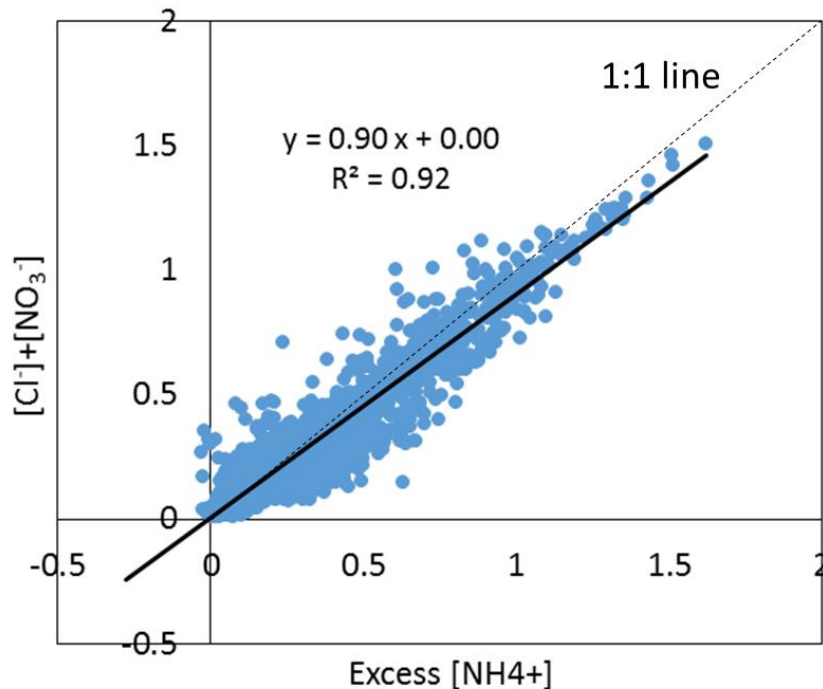
Assume  $[\text{NO}_3^-]/[\text{SO}_4^{2-}] = 0$ ,  $[\text{NH}_4^+]/[\text{SO}_4^{2-}] = 1.69$   
 as a critical value to determine a rich or poor  $\text{NH}_4^+$   
 environment.

city	value	author
Guangzhou	1.50	X Huang,2011
Shanghai	1.61	Y Shi,2012
Beijing	1.66	K He,2012

# Results and discussion

- Excess[NH<sub>4</sub><sup>+</sup>]

$$\text{Excess}[\text{NH}_4^+] = ([\text{NH}_4^+]/[\text{SO}_4^{2-}] - 1.69) * [\text{SO}_4^{2-}]$$



city	slope	author
Chongqing	0.65	K He,2012
Shanghai	0.86	Y Shi,2012
Beijing	0.95	K He,2012

Fig 14. Relationship between [NO<sub>3</sub><sup>-</sup>]/[Cl<sup>-</sup>] and Excess [NH<sub>4</sub><sup>+</sup>]

# Results and discussion

- $\text{NH}_4\text{NO}_3$  Gas-Particle Distribution

The mass concentration ratios of  $\text{HNO}_3/(\text{HNO}_3 + \text{NO}_3^-)$  and  $\text{HCl}/(\text{HCl} + \text{Cl}^-)$  can be evaluated to understand phase partitioning of these semi-volatile species (Du et al., 2010; Mehlmann and Warneck, 1995; Poschl et al., 2007). The higher  $\text{HNO}_3/(\text{HNO}_3 + \text{NO}_3^-)$  and  $\text{HCl}/(\text{HCl} + \text{Cl}^-)$  indicate that the semi-volatiles are more favored to exist as gas phase.

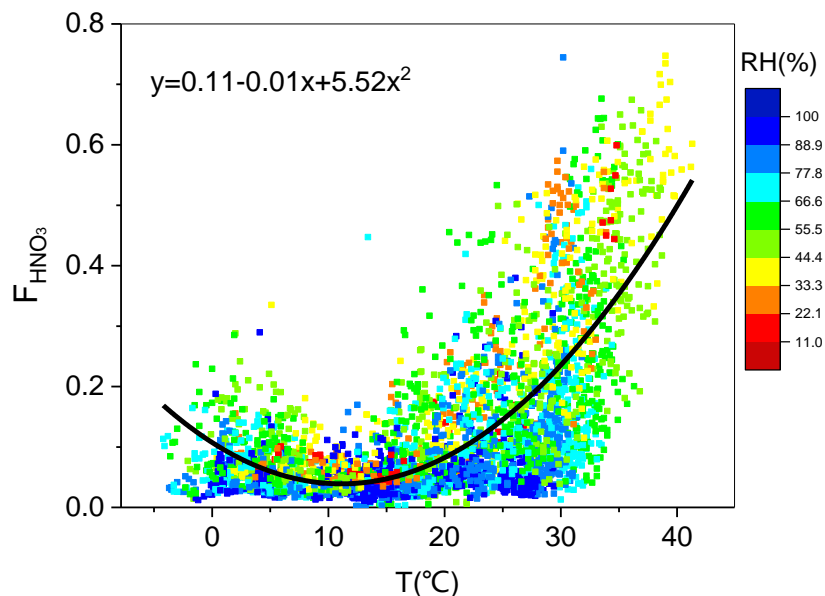


Fig 15. Relationship between  $F_{\text{HNO}_3}$  and  $T, \text{RH}$

# Results and discussion

- Diurnal variations

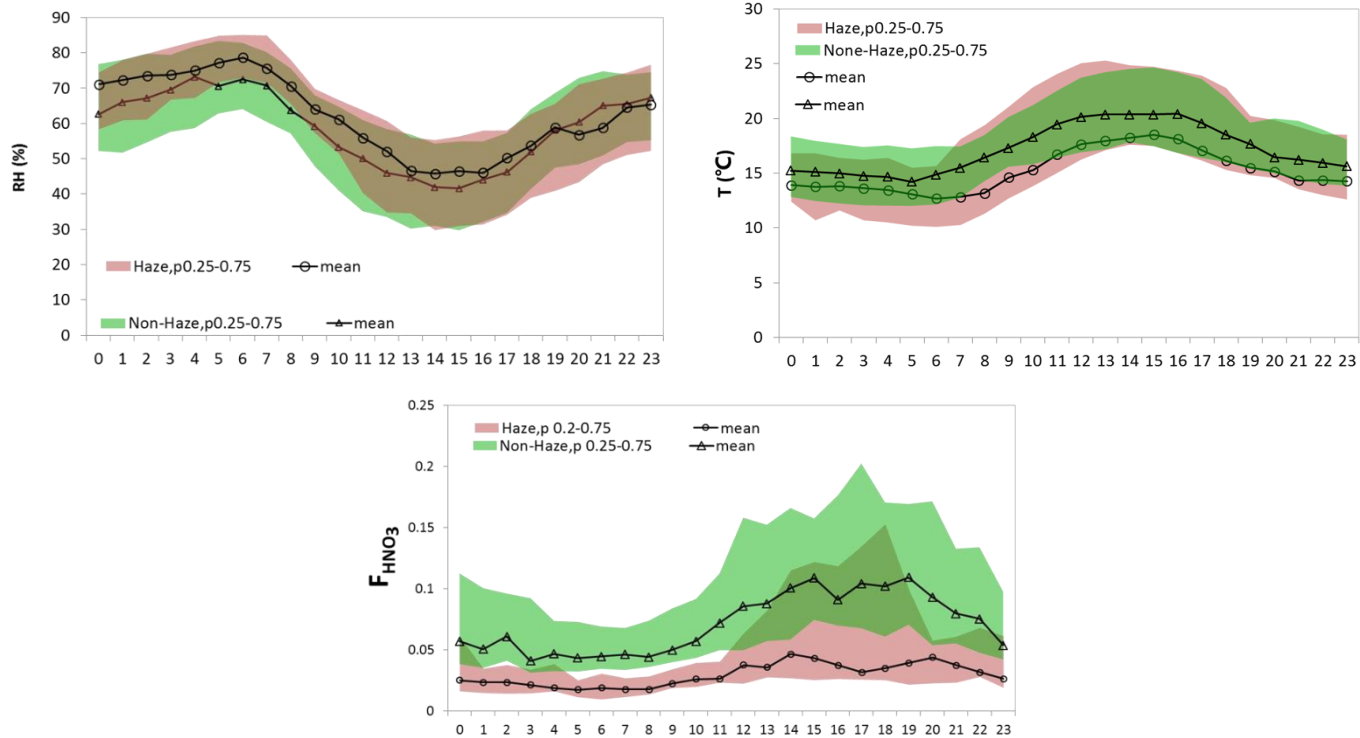


Fig 16. Diurnal variations of  $F_{\text{HNO}_3}$  and T, RH in haze and non-haze day

# Conclusions

- $\text{NH}_4^+$ 、 $\text{SO}_4^{2-}$ 、 $\text{NO}_3^-$  were the major ions accounting for 23.41%, 35.17% and 33.31% of TWSI, respectively.
- Seasonal variation of  $\text{PM}_{2.5}$  mass loading was winter>spring>summer. TWSI was the main component in  $\text{PM}_{2.5}$  in each season, with the average ranging from 64.12-81.96 $\mu\text{g}/\text{m}^3$ , contribution of  $\text{NO}_3^-$  showed an increase trend with the ascending  $\text{PM}_{2.5}$  mass concentration, exceeding that of  $\text{SO}_4^{2-}$  and become the major WSI in  $\text{PM}_{2.5}$ .
- SOR increased with elevated RH, indicating the important role of aqueous phase oxidation for  $\text{SO}_4^{2-}$  formation.
- $\text{NO}_3^-$ -and  $\text{Cl}^-$  mainly existed as  $\text{NH}_4\text{NO}_3$  and  $\text{NH}_4\text{Cl}$  in  $\text{PM}_{2.5}$ , which are semi-volatile. High temperature also facilitated the particle to gas partitioning, especially when  $T > 20^\circ\text{C}$ ,  $F_{\text{HNO}_3}$  is rapidly increased.